

A High-Efficiency Low-Wearing Hybrid Voltage Regulator for Utility Applications

YAFENG WANG ^{id} (Member, IEEE), AND TIEFU ZHAO ^{id} (Senior Member, IEEE)

Department of Electrical and Computer Engineering, University of North Carolina at Charlotte, Charlotte, NC 28223 USA

CORRESPONDING AUTHOR: YAFENG WANG (e-mail: ywang129@uncc.edu)

This work was supported by the Center for Advanced Power Engineering Research (CAPER).

ABSTRACT Step voltage regulator (SVR) has been utilized in power distribution systems for decades as the voltage regulation device. Due to the increasing integration of distributed energy resources, the conventional SVR is severely challenged by the modern power distribution pattern with high renewable energy penetration. The induced arc from the conventional SVR tap change and more frequent tap changes due to voltage instability from the renewable energy impose constraints on the conventional SVRs lifetime. Meanwhile, the conventional SVR device cannot regulate the voltage accurately since the SVR regulates the voltage step-by-step. This article proposed a hybrid voltage regulator with high-efficiency and low contact wearing, which can achieve arcless tap change and stepless voltage regulation by using a fractionally rated back-to-back power converter. The accurate load voltage regulation is guaranteed, while the tap changer mechanism remains in the system, which helps to promote the upgrade to the existing power distribution systems. The power converter capacity in the proposed topology is only 0.31% of the distribution transformer rating to achieve a stepless voltage regulation range of $\pm 10\%$, significantly reducing the system cost compared with the full power electronics solutions and projects high total system efficiency. The proposed hybrid voltage regulator was simulated and experimentally validated. The experimental results demonstrate arcless tap change operation and stepless voltage regulation. Collaborative operation between the conventional mechanical tap change and the power converter operation is also demonstrated to acquire large voltage regulation with fast-acting voltage control.

INDEX TERMS Arcless, converter, hybrid, stepless, step voltage regulator (SVR), tap changer, voltage regulation.

I. INTRODUCTION

Step voltage regulator (SVR) is a common voltage regulation equipment in the power distribution system to help compensate voltage fluctuation and variation and to regulate the grid voltage within the desired limits. The conventional SVR is an autotransformer-based configuration, as shown in Fig. 1, which has been implemented for decades [1], [2]. The voltage regulation is accomplished by moving the movable contacts to different tap positions, hence, to adjust the turns ratio of the transformer. The conventional tap change mechanism always generates an electric arc when the movable contact moves from the energized tap [3], [4], [5]. The conventional solution to the tap change arcing issue is to immerse the tap changer in the transformer oil tank along with the SVR. Contact erosion from the electric arc can significantly impact the SVRs

lifetime. Meanwhile, the electric arc causes carbon accumulation on the tap contacts and contaminates the transformer oil after a long time of operation.

In recent decades, more and more renewable energies, such as solar and wind energy, are being integrated with the power systems. The distributed pattern of renewable energy resources brings challenges to the conventional power system, which was originally designed for centralized power generation. The power generation fluctuation of distributed energy resources brings more instability and variability to the grid voltage and, thus, necessitates more fast-acting voltage control devices in the distribution system.

The pattern of modern power generation and renewable energy penetration requires more frequent tap change operations for the conventional SVRs, which imposes a further constraint

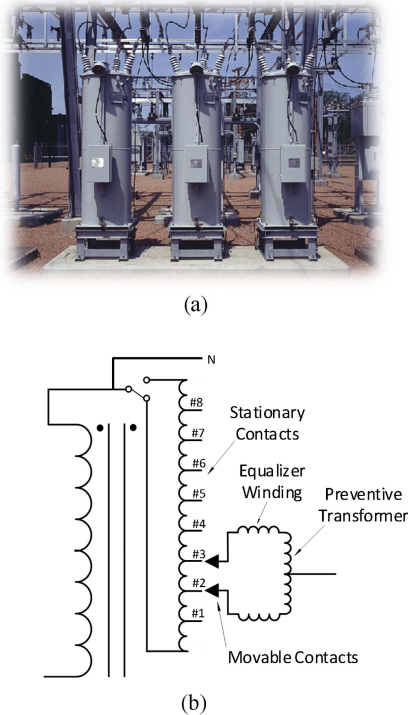


FIGURE 1. (a) SVRs in the substation. (b) Configuration of the conventional SVR.

on the SVRs lifetime [6], [7]. To extend the lifetime of the conventional SVRs, multiple studies have proposed different solutions to achieve arcless tap change. Arcless tap change solutions can be categorized into two types by the current conducting path, while the principles are both to eliminate the current in the tap-changing branch before the mechanical tap change operation. The first type is to cut off current in the tap-changing branch by using different types of switches. For example, vacuum switches are introduced as high-current circuit breakers and can be implemented for arc elimination of tap changes in [8]. But the vacuum chamber takes much space and is not suitable for occasions where installation space is limited. With the development of semiconductor devices, solid-state bidirectional switches are proposed to cut off current without arcing [9], [10], [11], [12], [13]. Hybrid switches are also proposed to lower down the conduction loss [14], [15]. However, these solutions require snubber circuits to deal with the hard-switching issue of semiconductor devices. Another type is to provide an alternative current path and redirect current to the path before the mechanical tap change. A study in [16] uses an active shunt diverter to redirect the current so that the energized contact separation can be avoided. But the topology still needs additional mechanical switches and other semiconductor switches, which makes the circuit complicated to operate and control. The arcless tap change solutions mentioned above primarily focus on cutting off current or redirecting current to the alternative path before the mechanical tap change and voltage is regulated step-by-step. The semiconductor devices are only utilized as switches.

The accurate voltage regulation with high resolution and fast voltage control is still not accomplished, which is not suitable for modern power systems with high renewable energy penetration where there are frequent voltage fluctuations.

Solid-state transformers (SSTs) in [17], [18], and [19] are proposed to regulate the full power or compensate the load voltage fluctuation, which can be accurate and continuous, through full-rating power electronics converter. The high power density of SST is also another advantage in applications with restricted space limit. However, the relatively lower efficiency of SST compared with the low-frequency transformer (LFT) makes it not realistic to be implemented in the distribution systems for continuous service. Although high-voltage SiC MOSFET enables SST for high-voltage applications to slightly increase the overall efficiency [20], reliability and necessary protection of medium-voltage converters are still challenges for SST [21]. Besides, the overall cost of SST is much higher than those of an equally rated LFT [22], [23], [24], [25]. Current research experiments on SST are primarily focused on lab-scale testing, while further long-term durability testings are required for SST to validate the reliability in the utility applications.

In most utility applications, voltage regulators are only required to regulate voltage deviation of $\pm 10\%$. To reduce the material cost and increase the system efficiency, hybrid transformer solutions are proposed where the power converter capacity is proportional to the voltage regulation range [26], [25], [26], [27]. Control schemes and system-level benefits by means of voltage control and active power control are also discussed in [28], [29], [30], [31], [32], and [33]. Smart transformer and hybrid transformer solutions in [28], [29], [30], [31], [32], and [33] help with power quality and voltage control, especially for modern distribution systems with high photovoltaic penetration. Based on the conventional distribution transformer, several innovative topologies are proposed in [34], [35], and [36] to regulate the grid voltage and to control the power delivery. Especially, designed filters are required for the proposed hybrid transformer topologies in [34], [35], and [36]. Hybrid transformer solutions reduce the material cost and increase the system efficiency compared with SST, but the tap changer mechanism in the conventional SVR is completely replaced by power converters, which is facing cost and reliability challenges in the existing power distribution systems.

It can be noticed from the previous literature review that arcless tap change mechanism, SST, and hybrid transformer require an individual set of devices to achieve the functions, respectively. Multiple issues of the conventional SVR need to be addressed, while the above-mentioned solutions lack connection and coordination with each other. There is a distinct gap between the arcless tap change solutions and SST/hybrid transformer solutions. To acquire a cost-effective and multifunctional retrofit of the existing power distribution transformer or SVR, the conventional tap change mechanism should be reserved and the power converter capacity requirement needs to be minimized, while the accurate and stepless

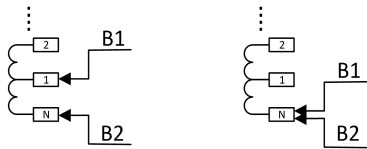


FIGURE 2. Bridging position (left) and nonbridging position (right).

voltage regulation and the arcless tap change functions can be realized by a single set of devices.

This article proposes a novel hybrid voltage regulator to bridge the gap between the arcless tap change solutions and solid-state/hybrid transformer solutions. The proposed hybrid voltage regulator can achieve both arcless tap change and stepless voltage regulation functions by using a fractionally rated (0.31%) back-to-back power converter. Meanwhile, high-efficiency and low contact wearing of the proposed hybrid voltage regulator ensure its feasibility in upgrading the existing power distribution systems.

The rest of this article is organized as follows. Section II describes the proposed hybrid voltage regulator and its components. Section III presents the operating principles of the arcless tap change operation and the stepless voltage regulation, including the circuit analysis and control algorithms. In Section IV, the arcless tap change operation and stepless voltage regulation functions are verified by the simulation results. Converter power loss simulation and system efficiency analysis are also presented. Section V presents the prototype hardware test results and performance evaluation. Finally, Section VI concludes this article.

II. PROPOSED VOLTAGE REGULATOR TOPOLOGY

As shown in Fig. 1, the conventional SVR consists of the main transformer, preventive transformer, equalizer windings, and the tap change mechanism. The two movable contacts have two positions, as shown in Fig. 2, where B1 and B2 represent the upper and lower branch. The preventive transformer acts as a mutual inductance to suppress the circulating current in the branch loop. The upper and lower branches share the load current equally. The equalizer windings are on the same magnetic core of the main transformer to balance the preventive transformer duty under the bridging and nonbridging positions.

The reference SVR model, as shown in Fig. 1(b), has eight taps in total and a neutral connector position. And between each two taps, there is a bridging position, as shown in Fig. 2, left that provides the middle-point voltage between the two taps. Considering the SVR tapped windings have two polarities, there are totally 32 voltage steps (± 16 voltage steps) for the conventional SVR, which provides $\pm 10\%$ voltage regulation range of the source voltage per the utility application standard. The relationship between the parameters is generalized by (1), where $V_{\text{step}(\%)}$ is the voltage percentage between each voltage step, V_{source} is the source voltage, V_{range} is the SVR voltage regulation range, and N is the number of taps. The reference SVR model has 10% voltage regulation range

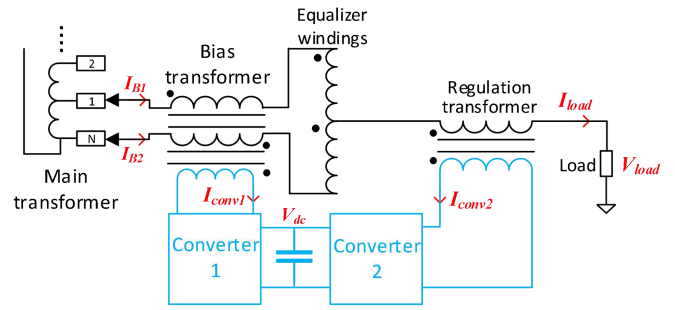


FIGURE 3. Proposed hybrid voltage regulator with a fractionally rated power converter.

with eight taps. Therefore, the voltage percentage between each step is 0.62% (5/8%), which is calculated by the following equation:

$$v_{\text{step}(\%)} = \frac{v_{\text{range}}}{v_{\text{source}} * 2N}. \quad (1)$$

The proposed hybrid voltage regulator topology is illustrated in Fig. 3. The hybrid voltage regulator combines the conventional SVR with a fractionally rated power converter. Additional winding is added to the preventive transformer to become the bias transformer. The regulation transformer is connected in series with the load to compensate for the load voltage. The back-to-back converter, which consists of Converter 1 and Converter 2 in Fig. 3, can handle bidirectional power flow to support different functional requirements.

The principle of arcless tap change is that the target branch current needs to be suppressed to zero before mechanical tap change to avoid an electric arc. The equivalent circuits of the branch loop are illustrated in Fig. 4. Equalizer winding voltages are $V_{\text{eq}1}$ and $V_{\text{eq}2}$. $V_{\text{bias}1}$ and $V_{\text{bias}2}$ are the bias winding voltages. V_{tap} represents the voltage between adjacent taps. The bias transformer also acts as a mutual inductor to suppress the circulating current in the branch loop. The leakage inductances of the upper and lower branch are L_{B1} and L_{B2} , respectively. The circulating current always exists due to the voltage difference in the branch loop. The bias transformer acts as a mutual inductor to suppress the circulating current. L_{M21} and L_{M12} are the equivalent mutual inductances between the two windings of the bias transformer. Converter 1 is connected to the third winding of the bias transformer and $V_{\text{conv}1}$ is the input voltage of Converter 1. Converter 2 is connected to the regulation transformer and $V_{\text{conv}2}$ is the output voltage of Converter 2. V_{reg} is the injected voltage for the load voltage regulation. The voltage before the regulation transformer is V'_{load} . V_{load} and I_{load} are the load voltage and current, respectively.

When Converter 1 works to suppress the branch current to zero in the arcless tap change operation, the required output voltage polarities of the Converter 1 are opposite for the bridging and nonbridging positions. The power flow directions of Converter 1 are also opposite at the two positions. The current distribution difference between B1 and B2 determines the power flowing through Converter 1. The compensation for

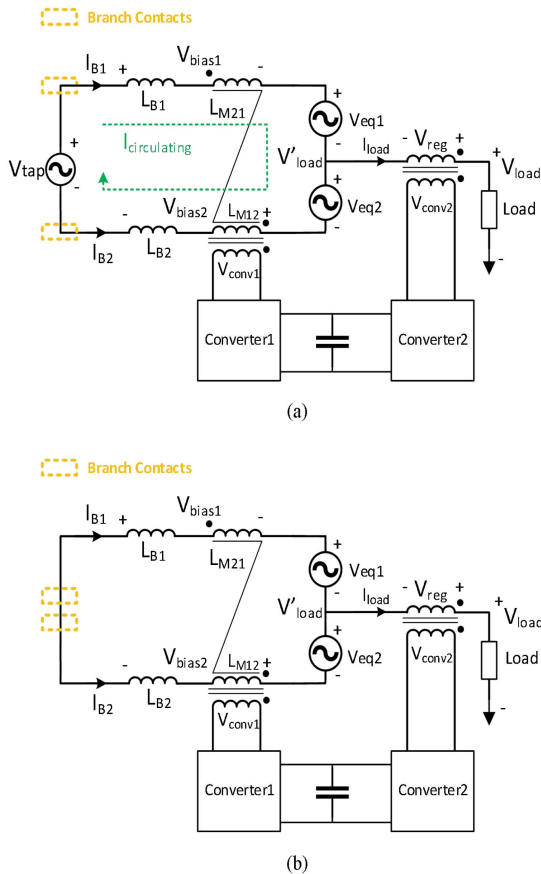


FIGURE 4. Equivalent circuits. (a) Bridging position. (b) Nonbridging position.

voltage sag and swell also requires Converter 2 to have two opposite power flow directions. Under the voltage regulation mode, Converter 1 works as the rectifier and Converter 2 operates as the inverter to compensate for the load voltage. Under the arcless tap change mode, Converter 2 works as the rectifier instead to support Converter 1, which serves as the inverter, to suppress the branch current. For this reason, Converter 1 and Converter 2 can provide power for each other under different operation modes. Both arcless tap change operation and stepless voltage regulation can be achieved with a fractionally rated back-to-back power converter. Converter 1 and Converter 2 are designed only to compensate half of the step voltage, which is 0.31% of the SVRs output voltage. The voltage compensation percentage is designed based on the voltage step ratio to bridge the gap between each voltage regulation step, which is ± 0.5 voltage step ($\pm 0.31\%$). At the voltage regulation transformer side, the current flowing through the transformer is the load current. So, converter is rated at 0.31% maximum transformer power rating. The ratio is only related to the voltage ratio between the regulation voltage range and the full load voltage. Therefore, the converter power ratings can be minimized to reduce the cost and efficiency impact to the traditional SVR system.

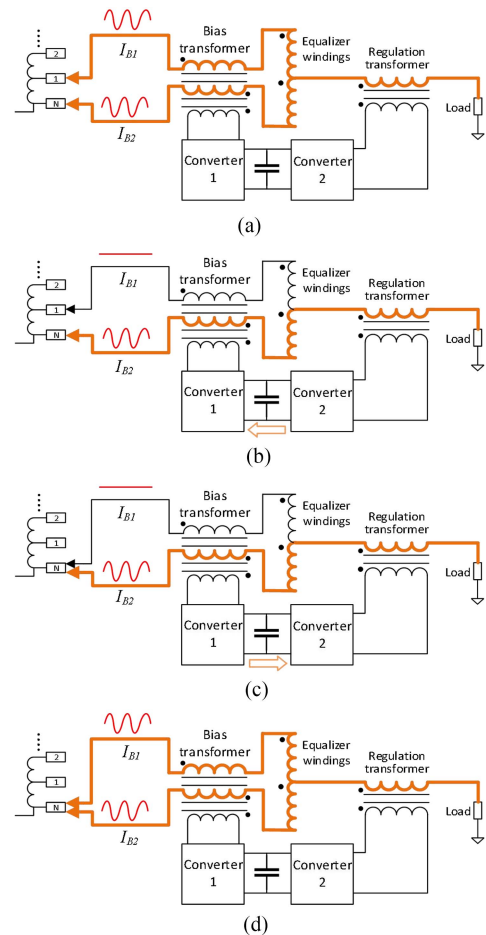


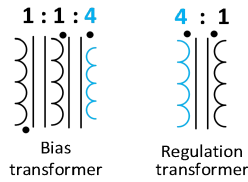
FIGURE 5. Arcless tap change operation sequence. (a) Converter 1 is disabled and Converter 2 regulates the dc bus voltage. (b) Upper branch current suppression. (c) Upper branch contact moves from tap 1 to tap N . (d) Converter 1 is shut down.

III. ARCLESS TAP CHANGE AND STEPLESS VOLTAGE REGULATION

A. ARCLESS TAP CHANGE OPERATION

To achieve the arcless tap change, the current in the target branch needs to be suppressed to zero before the mechanical tap change. Therefore, the arc can be eliminated when the metal contacts separate and the contact erosion rate can be significantly reduced. Fig. 5 illustrates a tap change sequence where the upper branch contact moves from tap 1 to tap N . The specific operations in Fig. 5(a)–(d) are described below. Current flowing paths are highlighted with thick orange lines.

- 1) Converter 1 is disabled and there is no current flowing at the input. Converter 2 works actively with current flowing through the regulation transformer to hold the dc bus voltage and avoid regulation transformer from core saturation.
- 2) Converter 1 starts to work and suppress the upper branch current I_{B1} to zero. The arrow between the two converters indicates the power flow direction.


FIGURE 6. Transformer turns ratio.

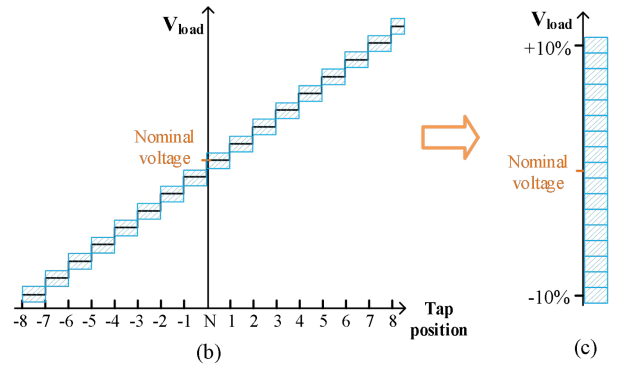
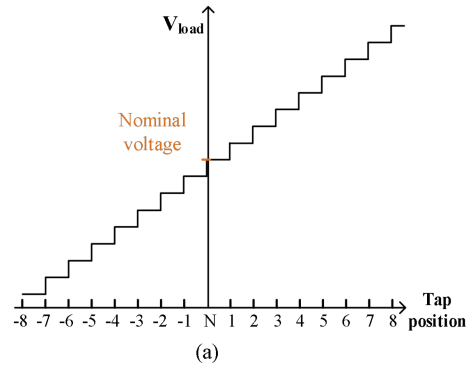
- 3) Upper branch contact moves from tap 1 to tap N without arc, while Converter 1 keeps working to ensure there is no current flowing through the upper branch. The power flow direction of the power converter is reversed, so the output voltage polarity on the regulation transformer is also reversed.
- 4) Converter 1 is shut down and the two branches share the load current again.

B. STEPLESS VOLTAGE REGULATION

In the proposed solution, the mechanical tap changer still makes tap changes to regulate large voltage steps, and the power converter injects a compensation voltage to adjust small voltage deviation between taps. As indicated in Fig. 5(b) and (c), the power flow direction is reversed from the bridging to the nonbridging position. The current distribution difference between the upper and lower branches also requires different values of the power supplied from Converter 1. For the same reason, the power supplied to or absorbed from Converter 1 can also be utilized for Converter 2 to output different voltage to the regulation transformer. Based on the transformer turns ratio design, as shown in Fig. 6, there is certainly a regulation voltage range from Converter 2, but the output voltage from the regulation transformer can bridge the gap between each step voltage change. Fig. 7(a) illustrates the conventional SVR load voltage relationship with the tap position where the load voltage is changed step-by-step for fixed source voltage. In the proposed hybrid voltage regulator, the voltage regulation range for each tap position is from negative to positive half step voltage as the blue-shaded area in Fig. 7(b). The regulation ranges for each tap position eventually combine into a continuous and stepless load voltage regulation range of $\pm 10\%$, as shown in Fig. 7(c).

C. CIRCUIT ANALYSIS AND CONTROL

All the parameter and variable definitions are described in Section II and labeled in Fig. 4. Based on the system design and transformer turns ratio in Fig. 6, the winding voltages of the bias transformer is expressed by (2). The equalizer winding voltages are designed to be a quarter of the tap voltage as (3). For each tap change operation, only one tap contact moves to the other tap, so the two tap contacts are either at the bridging position or the nonbridging position. Therefore, the step voltage change V_{step} is half of the tap voltage V_{tap} as (4). Due to the existence of the circulating current in the branch loop, the upper and lower branches do not share exactly half


FIGURE 7. Load voltage regulation principle for fixed source voltage V_s . (a) Conventional SVR with step voltage change. (b) Proposed hybrid voltage regulator with positive and negative half step voltage regulation range for each tap position. (c) Full range of the proposed stepless voltage regulation.

of the load current. So, the upper branch current I_{B1} and lower branch current I_{B2} are derived as (5) and (6), respectively. The load current is the sum of I_{B1} and I_{B2} , as shown in (7). The injected voltage from the regulation transformer, V_{reg} , regulates the load voltage to the nominal value as (8)

$$v_{\text{bias1}} = v_{\text{bias2}} = \frac{1}{4} v_{\text{conv1}} \quad (2)$$

$$v_{\text{eq1}} = v_{\text{eq2}} = \frac{1}{4} v_{\text{tap}} \quad (3)$$

$$v_{\text{step}} = \frac{1}{2} v_{\text{tap}} \quad (4)$$

$$i_{B1} = \frac{1}{2} i_{\text{load}} + i_{\text{circulating}} \quad (5)$$

$$i_{B2} = \frac{1}{2} i_{\text{load}} - i_{\text{circulating}} \quad (6)$$

$$i_{\text{load}} = i_{B1} + i_{B2} \quad (7)$$

$$v_{\text{load}} = v'_{\text{load}} + v_{\text{reg}}. \quad (8)$$

When two tap contacts are at the bridging position, as shown in Fig. 4(a), the voltage sum of bias windings and equalizer windings is equal to the tap voltage as (9). By solving (2), (3), and (9), bias winding voltages are derived as (10).

The circulating current can be expressed as (11)

$$v_{\text{tap}} = v_{\text{bias1}} + v_{\text{bias2}} + v_{\text{eq1}} + v_{\text{eq2}} \quad (9)$$

$$i_{\text{bias1}} = v_{\text{bias2}} = \frac{1}{4} v_{\text{tap}} \quad (10)$$

$$i_{\text{circulating}} = \frac{1}{2} v_{\text{tap}} / \omega (L_{B1} + L_{B2} + L_{M21} + L_{M12}). \quad (11)$$

When two tap contacts are at the nonbridging position, as shown in Fig. 4(b), the bias winding voltages are equal to the equalizer winding voltages in a reverse polarity as (12). By solving (2), (3), and (12), bias winding voltages are derived as (13). The circulating current can be expressed as (14) and it is in the reverse polarity of which in the bridging position

$$v_{\text{eq1}} + v_{\text{eq2}} = -(v_{\text{bias1}} + v_{\text{bias2}}) \quad (12)$$

$$v_{\text{bias1}} = v_{\text{bias2}} = -\frac{1}{4} v_{\text{tap}} \quad (13)$$

$$i_{\text{circulating}} = -\frac{1}{2} v_{\text{tap}} / \omega (L_{B1} + L_{B2} + L_{M21} + L_{M12}). \quad (14)$$

For the arcsless tap change operation, Converter 1 does not change the voltage distribution in the branch loop but regulates the target branch current to zero by injecting current through the connected winding of the bias transformer under current control mode.

For the load voltage regulation, the maximum and minimum voltage injections to the load are analyzed by the power balance law between two power converters. When the load power factor is unity, only the active power delivered between two converters is used for the load voltage regulation, which also applies to most SVRs in the distribution system. Since all winding voltages in the branch loop are in phase with the source and load voltages, the circulating current only affects the reactive power and it can be neglected for converter active power analysis.

When all the load currents flow through the upper branch, the active power absorbed by Converter 1 is expressed as (15). The voltage and current relationships of the regulation transformer windings are expressed by (16) and (17) based on the turns ratio. Hence, the active power of Converter 2 is expressed as (18). Because of the power balance between two converters as (19), the maximum injected regulation voltage is derived as (20) by solving (15), (18), and (19).

When all the load currents flow through the lower branch, the active power generated by Converter 1 is expressed as (21). By solving (18), (19), and (21), the minimum injected regulation voltage is derived as (22)

$$P_{\text{conv1}} = v_{\text{bias1}} i_{B1} = v_{\text{bias1}} i_{\text{load}} = \frac{1}{4} v_{\text{tap}} i_{\text{load}} \quad (15)$$

$$v_{\text{conv2}} = 4v_{\text{reg}} \quad (16)$$

$$i_{\text{conv2}} = \frac{1}{4} i_{\text{load}} \quad (17)$$

$$P_{\text{conv2}} = v_{\text{conv2}} i_{\text{conv2}} = v_{\text{reg}} i_{\text{load}} \quad (18)$$

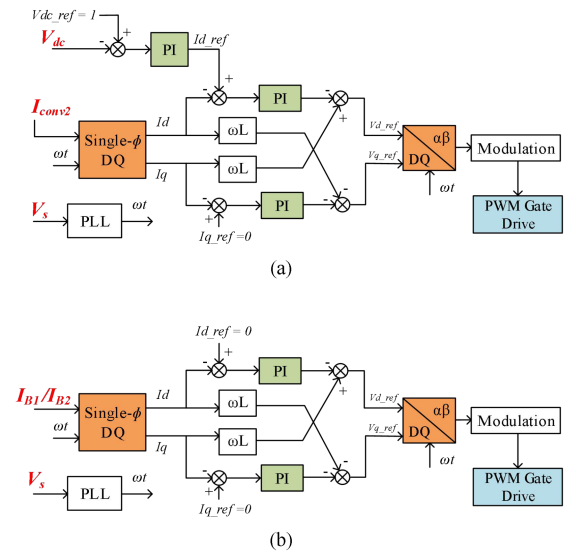


FIGURE 8. Arcless mode. (a) Converter 2 control. (b) Converter 1 control.

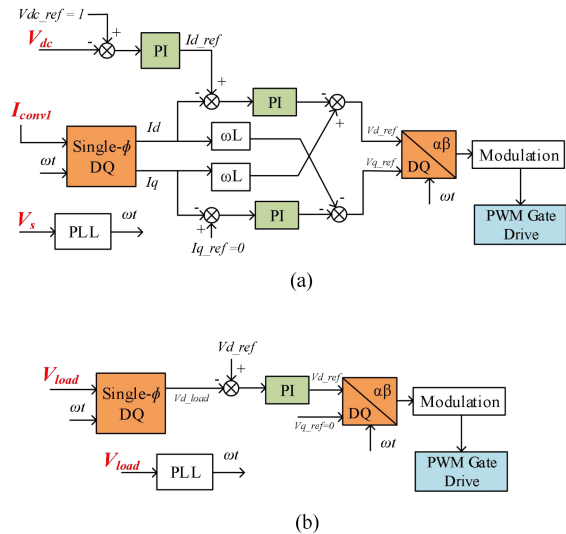


FIGURE 9. Regulation mode. (a) Converter 1 control. (b) Converter 2 control.

$$P_{\text{conv1}} = P_{\text{conv2}} \quad (19)$$

$$v_{\text{reg_max}} = \frac{1}{4} v_{\text{tap}} = \frac{1}{2} v_{\text{step}} \quad (20)$$

$$P_{\text{conv1}} = -v_{\text{bias2}} i_{B2} = -v_{\text{bias2}} i_{\text{load}} = -\frac{1}{4} v_{\text{tap}} i_{\text{load}} \quad (21)$$

$$v_{\text{reg_min}} = -\frac{1}{4} v_{\text{tap}} = -\frac{1}{2} v_{\text{step}}. \quad (22)$$

Two different control strategies are implemented for two converters under the arcsless mode and the regulation mode. Figs. 8 and 9 illustrate the control algorithms for two converters under the arcsless mode and regulation mode, respectively. Parameter names in the control diagrams are also marked in

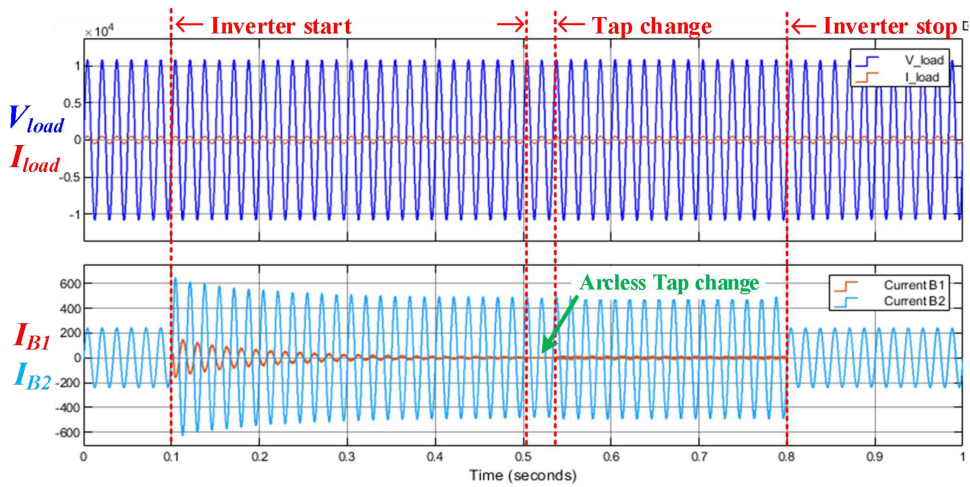

FIGURE 10. Arcless tap change mode simulation results.

TABLE 1. Simulation Specifications

Source voltage	7620 V
System rated power	2.6 MVA
Tap voltage (V_{tap})	96 V
Equalizer winding voltage (V_{eq})	24 V
Bias winding voltage (V_{bias})	24 V
Converter regulation voltage range	± 24 V
DC bus voltage	400 V
Converter capacity	8.16 kVA (0.31% of system rating)
Converter switching frequency	10 kHz

red in Fig. 3 correspondingly. V_s is the source voltage. V_{dc} is the dc bus voltage. I_{conv1} and I_{conv2} are the input currents of Converter 1 and Converter 2. I_{B1} and I_{B2} are the upper and lower branch currents. V_{load} is the load voltage. Fig. 8 focuses on the arcless mode that suppresses the target branch current to zero before the mechanical tap change. So, Converter 2 only regulates the dc bus voltage with unity power factor and Converter 1 controls the target branch current to zero with both I_{d_ref} and I_{q_ref} reference of zero. Circulating current can also be suppressed in this mode. Fig. 9 shows control algorithms for stepless load voltage regulation. Under the regulation mode, Converter 1 works as the rectifier to regulate the dc bus voltage, while Converter 2 works as the inverter to compensate the load voltage to the nominal value. So, only d -axis reference voltage V_{d_ref} is required in Converter 2 control block diagram to ensure that Converter 2 output voltage is in-phase with the load voltage. Converter 1 regulates the dc bus voltage with unity power factor, which does not affect the circulating current. And the circulating current does not affect or contribute to the active power control and the load voltage in-phase regulation. Different powers drawn from the

bias transformer lead to different branch current distribution for I_{B1} and I_{B2} .

IV. SIMULATION RESULTS

The full-scale simulation model of the device is developed in MATLAB/Simulink. The simulation parameters are listed in Table 1. For the standard SVR ratings, the distribution voltage is 7620 V, the transformer power rating is 2.6 MVA, and the voltage regulation range is $\pm 10\%$ with ± 8 taps in total. Every step voltage change is 48 V, which is half of the tap voltage. The proposed hybrid voltage regulator only requires 8.16 kVA converter capacity to cover the gap between each step voltage, which is 0.31% of the distribution transformer rating in the proposed hybrid voltage regulator.

A. SIMULATIONS FOR OPERATION VALIDATION

Fig. 10 shows the simulation results of a successful arcless tap change operation replicating the operation sequence, as shown in Fig. 5. The inverter, which is Converter 1 in the arcless tap change operation, starts to work at 0.1 s. The upper branch current I_{B1} is suppressed to zero before and after the mechanical tap change that happens at 0.5 s and ends at 0.54 s. The tap starts to move at 0.5 s when the upper branch current is suppressed to zero so that the arc can be eliminated for the mechanical tap change, which presents the successful arcless tap change operation. The upper branch current I_{B1} keeps being suppressed to zero after the mechanical tap change to avoid possible tap contact bouncing arc. And the load current flows entirely through the lower branch. Converter 1 is disabled at 0.8 s. Arcless tap change operation is completed.

System performance under the voltage regulation mode is presented in Fig. 11. To verify the stepless voltage regulation function, the output voltage of Converter 2 through the regulation transformer (V_{reg}) is commanded to increase linearly from -24 to $+24$ V from 0.5 to 1.5 s. The two tap contacts are at the nonbridging position. Converter 1 works as the rectifier to provide power for Converter 2 under the regulation mode.

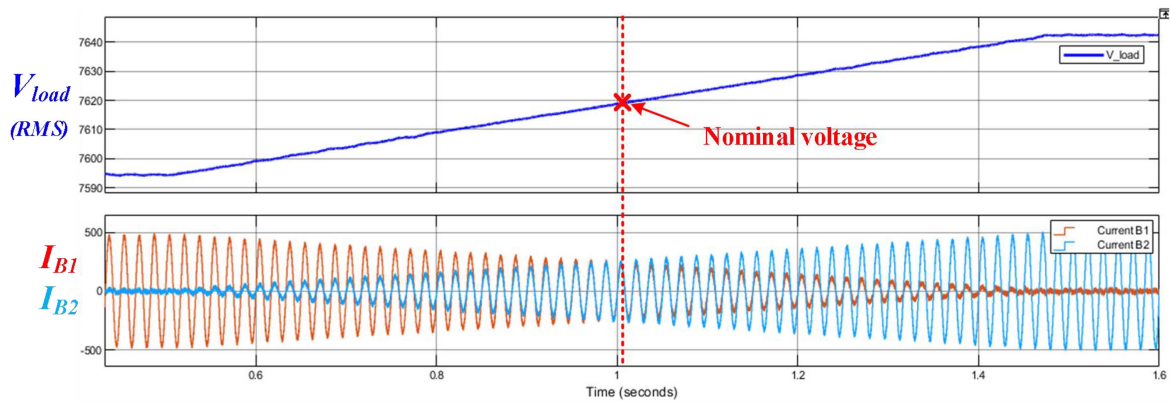


FIGURE 11. Voltage regulation mode simulation results.

Fig. 11 demonstrates that the load voltage can be regulated continuously from negative to positive half step voltage during the voltage ramping-up. Therefore, the stepless voltage regulation is achieved by the power converter injecting regulation voltage in series with the load. At 1 s, the load voltage reaches the nominal voltage of 7620 V at the nonbridging position. When load voltage increases, the branch currents have different distributions as I_{B1} decreases and I_{B2} increases, which indicates the power flow change from the bias transformer. When the load voltage is below the nominal tap voltage before 1 s, Converter 1 absorbs active power from Converter 2 and I_{B2} is larger than I_{B1} . When the load voltage is higher than the nominal tap voltage after 1 s, Converter 1 generates active power from the bias transformer and supplies it to Converter 2 and I_{B1} becomes larger than I_{B2} . Zoom-in waveforms of Converter 1 and the upper branch current I_{B1} are presented in Fig. 12. When Converter 1 absorbs active power from Converter 2, the phases of Converter 1 voltage and current are opposite and I_{B1} is larger than I_{B2} . In Fig. 12(a), Converter 1 is at maximum reverse power flow before 0.5 s and the upper branch current I_{B1} is at its maximum peak value of 480 A. When Converter 1 generates active power to Converter 2, Converter 1 voltage and current are in-phase and I_{B1} is less than I_{B2} . In Fig. 12(b), Converter 1 is at maximum forward power flow after 1.5 s and the upper branch current I_{B1} is at its minimum value of almost zero. The residual current in the upper branch is the circulating current. It is verified that different current distribution in the upper and lower branches can provide power for the load voltage regulation. In short, the two converters can support each other to achieve both arcless tap change and stepless load voltage regulation.

B. COLLABORATIVE OPERATION OF POWER ELECTRONICS VOLTAGE REGULATION AND MECHANICAL ARCLESS TAP CHANGE

When a more significant voltage deviation ($>1/2 V_{\text{step}}$) is detected, the collaborative operation between the power electronic converter and the mechanical tap change becomes

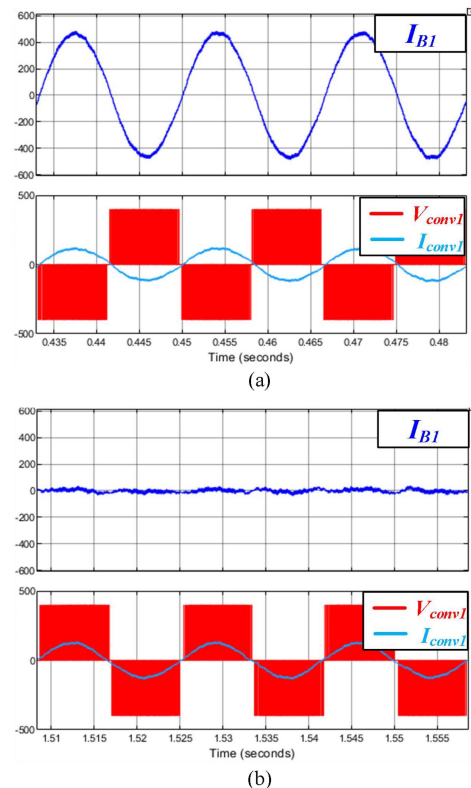


FIGURE 12. (a) Zoom-in waveforms before 0.5 s when Converter 1 is at maximum reverse power flow. (b) Zoom-in waveforms after 1.5 s when Converter 1 is at maximum forward power flow after 1.5 s.

indispensable. Power electronics voltage regulation by Converter 2 is implemented for small voltage deviation within ± 0.5 step voltage. When the voltage deviation is beyond the regulation capability of Converter 2, an arcless tap change command is conducted to acquire a larger voltage regulation range. Fig. 13 shows a collaborative operation simulation of voltage bucking and arcless tap change to regulate the load voltage back to the nominal voltage of 7620 V. Two tap contacts were previously at the bridging position when upper

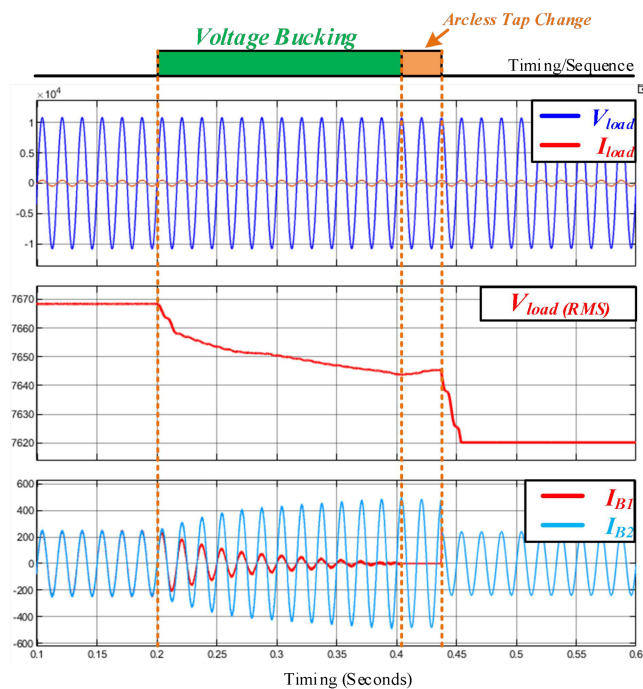


FIGURE 13. Collaborative operation simulation of power electronics voltage regulation and mechanical arcless tap change.

branch connects with tap #1 and lower branch connects with tap N . Converter 2 works to lower the load voltage and the active power flows from Converter 2 to Converter 1. The upper branch current I_{B1} decreases to around zero at 0.4 s, while the lower branch current I_{B2} increases. The branch current distribution at 0.4 s provides the necessary condition for the upper branch arcless tap change to lower down taps as the upper branch current I_{B1} is suppressed. After 0.4 s, a mechanical arcless tap change is implemented to lower down the upper branch contact from tap #1 to tap N . The load voltage is regulated to 7620 V nominal voltage, so the collaborative voltage regulation operation is completed.

Based on the previous circuit analysis and voltage regulation simulation, the voltage regulation range provided by the power electronics converter is within plus and minus half step voltage. Therefore, the collaborative operation of power electronics voltage regulation and arcless tap change is necessary to acquire larger voltage regulation when the load voltage variation is beyond the voltage regulation range limit of the converter.

C. CONVERTER POWER LOSS AND SYSTEM EFFICIENCY

Since the power converter in the proposed hybrid voltage regulator works continuously to regulate the load voltage, the system efficiency impact needs to be evaluated. Based on the simulation specifications in Table 1 and the transformer turns ratio design in Fig. 6, the 600 V, 120 A insulated gate bipolar transistor (IGBT) is selected as the device reference model [37]. The PLECS model of the selected IGBT is imported in

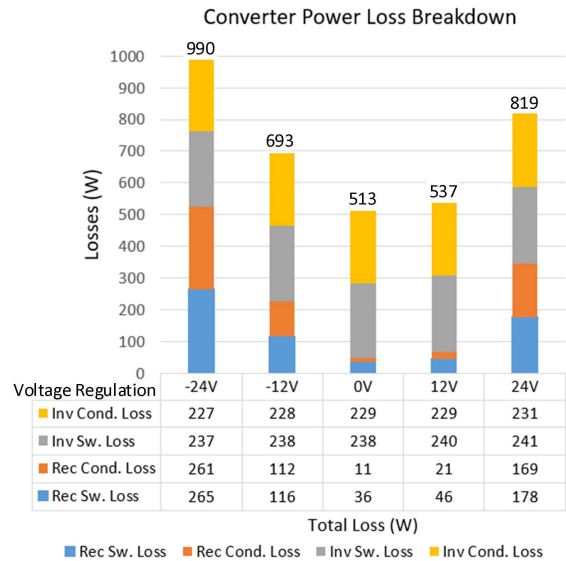


FIGURE 14. Converter power loss breakdown.

PLECS for converter power loss simulation. PLECS simulation uses similar mathematical modeling for electric circuits as MATLAB/Simulink and it is also capable of device loss and thermal simulation. The imported device PLECS model reflects the device switching and conduction losses simultaneously during the simulation by matching the device loss value accordingly with the instant device voltage, current, and temperature in a lookup table. The simulation conditions are the same as the parameters in Table 1. The steady-state IGBT case temperature is at 70 °C. The converter power loss is simulated for -24 V, -12 V, 0 V, 12 V, and 24 V load voltage regulation, respectively. Different load voltage regulations correspond to different converter powers and power flow directions.

Based on the PLECS simulation results, the converter power loss breakdown is shown in Fig. 14. For the load voltage regulation mode, Converter 1 is the rectifier, while Converter 2 serves as the inverter. Since the regulation transformer secondary side is coupled with the inverter (Converter 2) load current, the inverter conduction loss and switching loss do not change much when the load voltage regulation varies. However, the bias winding is a voltage source for Converter 1. The conduction loss and switching loss of the rectifier (Converter 1) change significantly when the load voltage regulation varies. The reason is that Converter 1 input current from the bias winding changes along with the load voltage regulation.

The simulated total system efficiency is presented in Fig. 15. The estimation assumes that the conventional SVR efficiency is 98%. Although the total converter power loss is up to 1 kW, the maximum converter power loss is less than 0.04% of the total system power. Therefore, the system efficiency impact from the power converter power loss can be negligible in the load voltage regulation. While the converter is at light-load condition with poor converter efficiency at zero load voltage regulation, the absolute power loss is at the

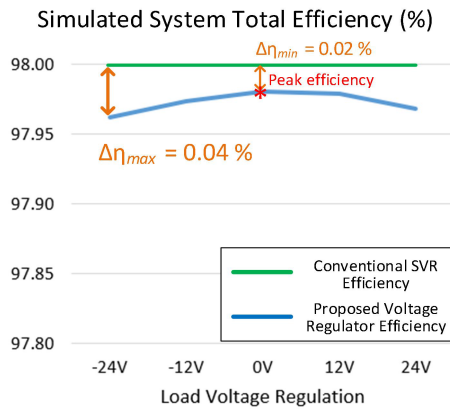


FIGURE 15. Simulated system total efficiency.

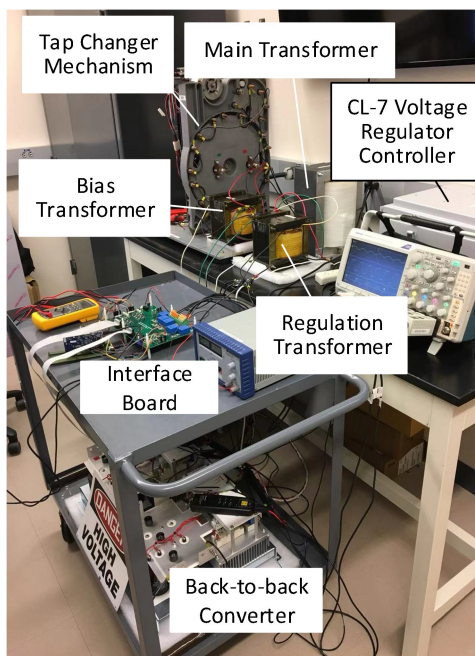


FIGURE 16. Proposed hybrid voltage regulator prototype.

minimum value for the system. So, the system peak efficiency of 97.98% happens at zero load voltage regulation condition, where the efficiency impact is only 0.02%.

V. HARDWARE TEST RESULTS

A scaled-down experimental platform is developed in the lab to evaluate the prototype performance, as shown in Fig. 16. The main transformer is a tap changer transformer. A tap changer mechanism and an Eaton CL-7 voltage regulator controller are utilized to make tap changes in the experiment. The source voltage is 240 V and the load is rated at 288 V, 10 A, and 3 kW. The power converter dc bus voltage is designed as 200 V as the maximum injected voltage at the inverter side is 96 V. Other detailed parameters of the scaled-down prototype test are listed in Table 2. It is noted that only the

TABLE 2. Prototype Test Specifications

Source voltage	240 V
Load voltage	288 V
Load current	10.5 A
Load power	3 kW
Tap voltage (V_{tap})	96 V
Equalizer winding voltage (V_{eq})	24 V
Bias winding voltage (V_{bias})	24 V
Regulation voltage range	± 24 V
Maximum required converter power/percentage of the system	250W/8.4%
DC bus voltage	200 V
Converter switching frequency	10 kHz

current rating and SVRs primary-side input voltage are scaled down in the experimental platform, while the tap voltage and other winding voltages are the same with the medium-voltage model, including the regulation voltage range. Therefore, the converter power percentage is 8.4% in the scaled-down prototype. A DSP TI 28379D controller is used to implement the proposed arcless tap change and voltage regulation control. An interface board is designed to communicate between the DSP controller and the power converter.

A. ARCLESS TAP CHANGE TEST

Arcless tap change function is validated first when Converter 2 operates as the rectifier to regulate the dc bus voltage and provides power for Converter 1. The hardware tests show the full operation process of arcless tap change in Fig. 17(a). When Converter 1 is started, the upper branch current I_{B1} is suppressed to zero after a few cycles and the lower branch current I_{B2} is doubled as the full load current is flowing through the lower branch. It can be observed that the upper branch current keeps being suppressed to zero before and after the tap change, which is contributed by the inverter output voltage compensation strategy proposed in [38]. As Converter 1 is disabled after the tap change, the upper and lower branch share the load current equally again and the load voltage lowers down to the next step range. The load voltage and current waveforms during the arcless tap change are shown in Fig. 17(b). After the mechanical tap change, the load voltage and current are lowered down. The upper and lower branch current distribution variation and the current rebalancing process do not affect the load voltage V_{load} and load current I_{load} sinusoidal waveforms.

B. ELECTRIC ARC IMPACT COMPARISON

To further evaluate the advantage of arcless tap change operation, the detailed electric arc impact comparison is shown in Fig. 18. The contact voltage $V_{contact}$ represents the voltage between the upper branch metal contact and the transformer tap contact. When tap contacts are separated from each other,

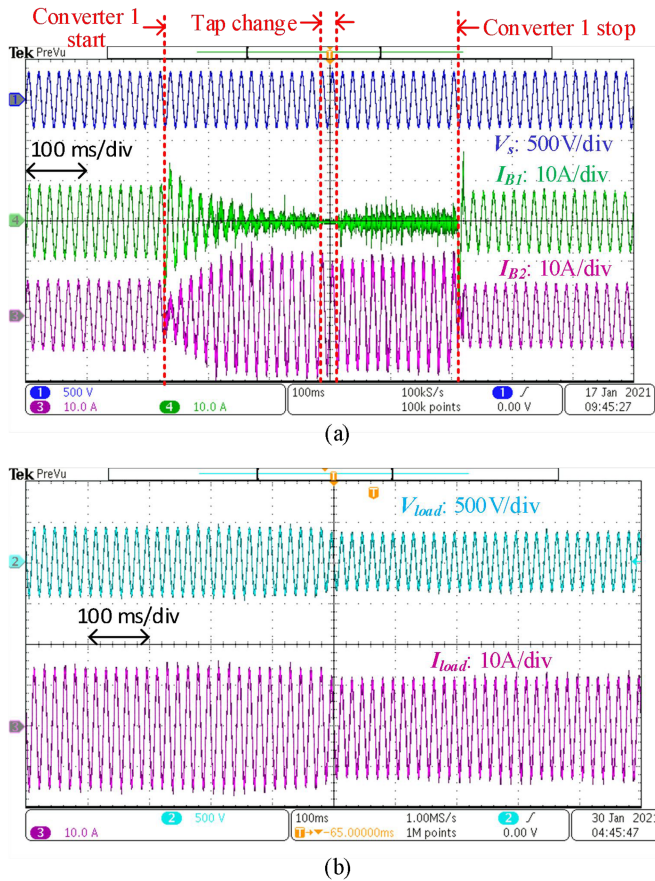


FIGURE 17. Arcless tap change waveforms. (a) Full operation process. (b) Load voltage and current waveform during the arcless tap change.

$V_{contact}$ changes from zero to a nonzero value. Therefore, the criteria to determine the existence of the electric arc is when both the contact voltage and the upper branch current I_{B1} are nonzero. And the electric arc in Fig. 18(a) and the sparks in Fig. 18(b) are indicated accordingly. In Fig. 18(b), I_{B1} is re-conducted after it first goes to zero and a few sparks also exist. The reason is that it takes a distance and a short time for two metal contacts to completely separate. And it is unavoidable to have the contact mechanical bouncing and reconnection during the mechanical tap separating movement.

The electric arc erosion rate of the contact metal materials can be quantified by (23) [39]. In (23), k_I is the erosion coefficient that varies for different materials, for example, k_I is 2.4 for copper. So, the electric arc impact comparison can be made based on the integration of $I^{1.6}$ when the contact voltage $V_{contact}$ is nonzero

$$dG/dt = k_I I^{1.6} \mu\text{g/s}. \quad (23)$$

The current data are collected from the oscilloscope and processed in MATLAB. And the ampere-second number of the $I^{1.6}$ integration is 0.077 A·s for the conventional tap change with arc and 7.3×10^{-5} A·s for the arcless tap change. Based on the scaled-down experiments, the contact erosion rate of the arcless tap change is significantly reduced by 1055

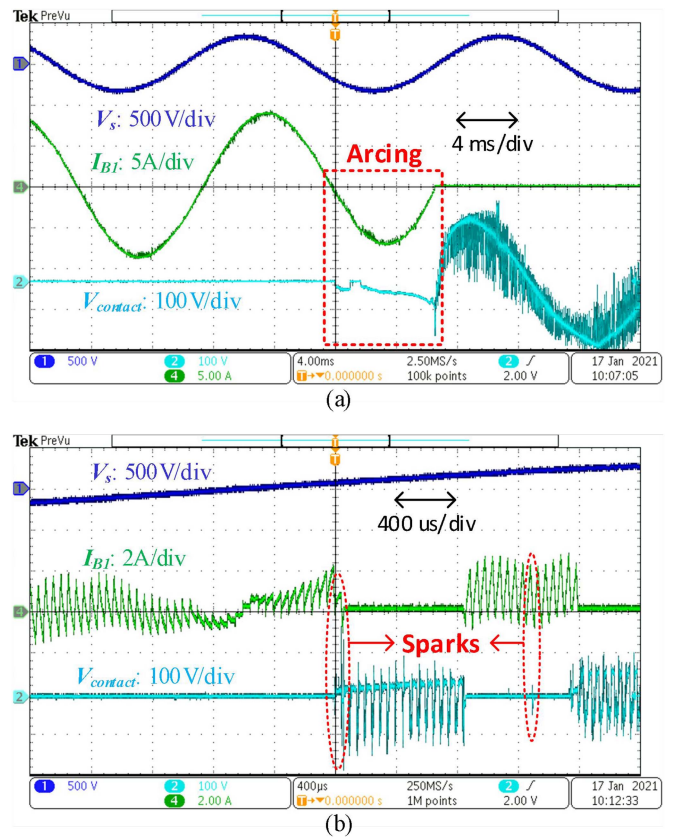


FIGURE 18. (a) Conventional SVR tap change waveform. (b) Arcless tap change waveform.

times compared with the conventional mechanical tap change with the arc. The erosion rate difference can be even more significant in the medium-voltage SVR since the load current is much higher than the scaled-down prototype and it is more difficult to extinguish the electric arc.

Therefore, the electric arc of the mechanical tap change is eliminated and the proposed arcless tap change operation is achieved successfully.

C. LOAD VOLTAGE REGULATION TEST

For the voltage regulation function, Fig. 19(a) illustrates that the load voltage V_{load} is regulated to 288 V, while the source voltage V_s ramps up from 220 to 260 V in 0.5 s. The equivalent load voltage variation is ± 24 V. The closed-loop control is achieved in the load voltage regulation hardware test. As the source voltage changes below and beyond the nominal value of 240 V, the injected regulation voltage changes from +24 to -24 V. It determines the power flow direction between the power converters, which eventually influences the current distribution in the upper and lower branches. Therefore, different I_{B1} and I_{B2} distribution can be observed as the source voltage changes. As indicated by the dashed line in Fig. 19(a), the source voltage increases from 220 to 260 V maximum value. When the source voltage is below 240 V, the upper branch current I_{B1} is larger than the lower branch current

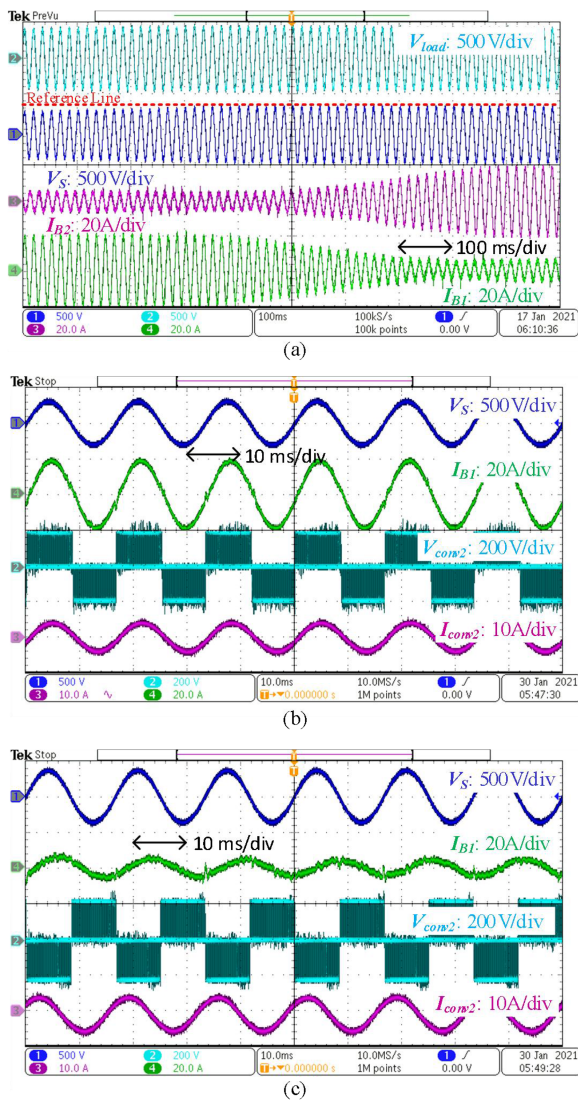


FIGURE 19. Voltage regulation waveforms. (a) Branch currents and voltage waveforms of the source and load. (b) Converter 2 waveforms when injecting positive voltage. (c) Converter 2 waveforms when injecting negative voltage.

I_{B2} and Converter 1 provides active power for Converter 2 to increase the load voltage to the nominal value of 288 V. When the source voltage is beyond 240 V, the upper branch current I_{B1} becomes smaller than the lower branch current I_{B2} and Converter 1 absorbs active power from Converter 2 as Converter 2 lowers down the load voltage to the nominal value of 288 V. The load voltage can be regulated continuously, while the source voltage varies continuously so long as it is within the regulation range. The residual currents of I_{B2} at the beginning of the voltage regulation process and I_{B1} at the end, respectively, are the circulating current in the branch loop, which is necessary to keep the voltage balance in the branch loop and the voltage between the two adjacent tap contacts. Fig. 19(b) and (c) are the zoom-in waveforms of Converter 2 voltage and current when the source is undervoltage and overvoltage, respectively. The different polarity of Converter

2 voltage and current indicates the opposite power flow directions of the converters under different voltage regulation conditions, where the branch current distribution also varies as seen from the upper branch current I_{B1} .

To further explain the circulating current in the branch loop, the waveforms in Fig. 19 are good evidence of the existence of the circulating current in the upper and lower branches. Circulating current is caused by the tap voltage across the loop inductance of the upper and lower branches, which is in-phase with the source and load voltage. So, the circulating current has 90° phase shift to the source voltage.

In Fig. 19(a), it is observed that I_{B1} is larger than I_{B2} when active power is drawn from the Converter 1 when Converter 2 injects positive voltage or active power to the load. Reversely, I_{B2} is larger than I_{B1} when Converter 2 injects negative voltage to or absorbs active power from the load. Based on this rule, we can summarize the behavior below.

In Fig. 19(b), Converter 2 injects positive voltage to the load. So, the upper branch current I_{B1} is the summation of the load current, which is in-phase, and the circulating current, which has 90° phase difference. The circulating current is less than 3 A in RMS value. And the load current is dominant in the upper branch current I_{B1} . Therefore, it is observed that I_{B1} is slightly phase shifted to the source voltage V_S . And the lower current I_{B2} is only the circulating current in this condition.

In Fig. 19(c), Converter 2 injects negative voltage to the load. So, the upper branch current I_{B1} is only the circulating current in this condition and is 90° phase shifted to V_S . However, I_{B2} is the summation of the load current and the circulating current, which is not shown in the waveform.

Based on the hardware test results, arless tap change operation and load voltage regulation function are both verified. And the experimental performance matches the simulation results of the full-scale system. The power flow direction and current distribution correspond to the circuit analysis under different operation modes and conditions.

D. PROTOTYPE TEST OF COLLABORATIVE OPERATION

Fig. 20 presents the prototype test results of a collaborative operation of power electronics voltage regulation and mechanical arless tap change. Two tap contacts were previously in the bridging position where the upper branch connects with tap #1 and the lower branch connects with tap N . At T_1 , the source voltage changes to 230 V, which is lower than the nominal load voltage of 240 V. The load voltage variation is beyond the limit of the voltage regulation range from Converter 2, so a collaborative operation is necessary in this case.

Converter 2 first regulates the load voltage from 288 to 264 V after T_1 . In the voltage bucking process between T_1 and T_2 , the upper branch current I_{B1} is lowered to around zero due to the reverse power flow from Converter 2 to Converter 1. Between T_2 and T_3 , an arless tap change is implemented to lower the upper branch contact from tap #1 to tap N . The arless tap change operation proceeds the voltage regulation to the lower range at the next tap position where two branches

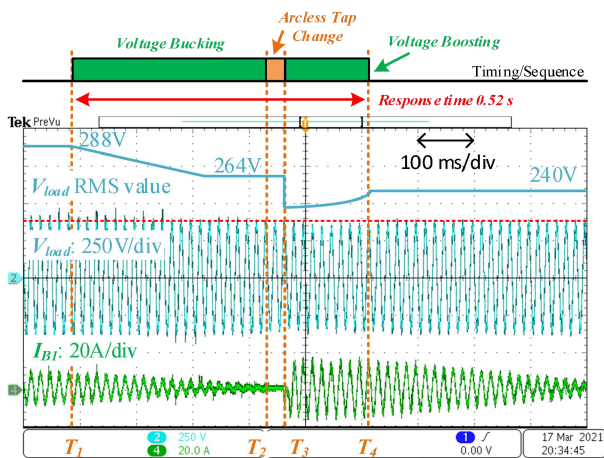


FIGURE 20. Prototype test waveforms of the collaborative operation.

both connect with tap N . After a voltage boosting process between T_3 and T_4 , the load voltage is regulated to the nominal voltage of 240 V. The collaborative operation is completed and the total response time is 0.52 s.

The prototype test verifies the collaborative operation of power electronics voltage regulation and arcless tap change. The operation is necessary to link all voltage regulation ranges at each tap positions and eventually combines into the accurate and stepless voltage regulation of $\pm 10\%$. The response time of 0.52 s is also faster than the conventional tap change of the SVR whose tap change response time takes several seconds.

In addition to the proposed functions, the back-to-back converter can be controlled to compensate the circulating current in the branch loop and also to implement var control to the load if it is within the converter's power capacity. This method can be further investigated and improved in the future research. Preliminary var control function is validated on the previous version of the prototype [38].

E. COMPARISON WITH EXISTING SOLUTIONS

Although hybrid transformers and SST are able to implement voltage regulation, high material cost and relatively low efficiency still make it hard for utility application and power infrastructure upgrade. The proposed hybrid voltage regulator has many advantages compared with the existing solutions in several aspects, especially for utility application and promotion for large-scale power infrastructure upgrade. Considering that the conventional SVR has been widely implemented in the existing power distribution systems for decades, it is difficult for utility operators to adopt a new technology that completely replaces the existing conventional SVR due to capital investment concern, reliability issue, and efficiency impact.

SST has many advantages than the conventional LFT and hybrid transformer, such as compact volume, full-range voltage control, and var compensation. Considering the fact that

the voltage regulation range is usually $\pm 10\%$ for voltage regulation devices in the distribution system, the SST solution with 100% full rating of voltage regulation is costly and unnecessary for conventional utility applications. For the conventional hybrid transformer with series voltage compensation, the power converter rating percentage is directly related with the required voltage regulation range. For example, 10% voltage regulation range for the conventional hybrid transformer requires the power converter rating to be 10% of the system total power. But the proposed hybrid voltage regulator reserves the tap changer mechanism in the system and the arcless tap change also extends the lifetime of tap changer mechanism. The Converter 2 only needs to compensate the voltage deviation between each tap, which minimizes the power electronics converter rating to 0.31% and reduces the material cost of power electronics' components compared with the hybrid transformer of 10% converter rating and SST. The accurate voltage regulation of $\pm 10\%$ is accomplished with the collaborative operation of arcless tap change and power electronics voltage regulation. Since the power converter capacity is minimized to 0.31% in the proposed solution, most power is delivered through the LFT. Power loss from the converter is also minimized with lowest efficiency impact on the proposed hybrid voltage regulator.

Due to the minimized capacity of the power converter in the proposed topology, the efficiency impact to the conventional tap changer is much smaller compared with SST and hybrid transformer. Reservation of the tap changer mechanism also helps retrofit numerous conventional SVRs in the existing distribution system with lower installation cost for utility operators.

To conclude, the proposed hybrid voltage regulator is a high-efficiency low-cost solution to achieve both arcless tap change and stepless voltage regulations. Longer operation lifetime, accurate voltage regulation, and high efficiency are the advantages of the proposed hybrid voltage regulator.

VI. CONCLUSION

In this article, a hybrid voltage regulator based on the conventional SVR and a fractionally rated power converter is proposed. An additional regulation transformer is implemented at the load side and an extra winding is added to the bias transformer. The new device achieves both arcless tap change and stepless voltage regulation functions. Simulation and experimental results verify that the electric arc can be eliminated when tap changes. This reduces the contact erosion rate by 1055 times and significantly extends the lifetime of the voltage regulator. Fast and accurate voltage regulations are also guaranteed by the proposed hybrid voltage regulator. Both functions are achieved by a back-to-back power converter with different control strategies, which are validated by the scaled-down experimental results. The power converter capacity of the proposed solution in the full-scale distribution system is only 0.31% of the distribution transformer power rating for SVR with ± 8 taps, which significantly reduces the additional power converter cost and achieves a high system

efficiency in the medium-voltage applications. The proposed solution requires minimal changes to the existing SVR but eliminates the arcing nature of these tap changers and achieves accurate and stepless load voltage regulation. The proposed solution will significantly enhance the reliability and lifetime of the voltage regulators, meanwhile improve the voltage fluctuations in the distribution system due to renewable integrations.

REFERENCES

- [1] Y. Wang and T. Zhao, "A hybrid voltage regulator with arclless tap change and stepless voltage regulation functions," in *Proc. IEEE Energy Convers. Congr. Expo.*, Detroit, MI, USA, 2020, pp. 4857–4863.
- [2] Y. Wang, "Power electronics assisted voltage regulators for modern distribution systems," Ph.D. dissertation, College Eng., Univ. North Carolina Charlotte, Charlotte, NC, USA, 2021.
- [3] R. Jongen, E. Gulski, K. Siodła, J. Parciak, and J. Erbrink, "Diagnosis of degradation effects of on-load tap changer in power transformers," in *Proc. ICHVE Int. Conf. High Voltage Eng. Appl.*, Poznan, 2014, pp. 1–4.
- [4] J. J. Erbrink et al., "Diagnosis of onload tap changer contact degradation by dynamic resistance measurements," *IEEE Trans. Power Del.*, vol. 25, no. 4, pp. 2121–2131, Oct. 2010.
- [5] G. L. Quinton, "Advantages of an arclless voltage regulator," *IEEE Trans. Ind. Appl.*, vol. IA-20, no. 2, pp. 425–428, Mar. 1984.
- [6] G. K. Ari and Y. Baghzouz, "Impact of high PV penetration on voltage regulation in electrical distribution systems," in *Proc. Int. Conf. Clean Elect. Power*, Ischia, Italy, 2011, pp. 744–748.
- [7] A. Hariri, M. O. Faruque, R. Soman, and R. Meeker, "Impacts and interactions of voltage regulators on distribution networks with high PV penetration," in *Proc. North Amer. Power Symp.*, Charlotte, NC, USA, 2015, pp. 1–6.
- [8] D. Dohnal and B. Kurth, "Vacuum switching, a well proven technology has found its way into resistance-type load tap changers," in *Proc. IEEE/PES Transmiss. Distrib. Conf. Expo.*, Atlanta, GA, USA, vol. 1, 2001, pp. 161–165.
- [9] S. Martinez Garcia, J. C. Campo Rodriguez, J. A. Jardini, J. Vaquero Lopez, A. Ibarzabal Segura, and P. M. Martínez Cid, "Feasibility of electronic tap-changing stabilizers for medium voltage lines—Precedents and new configurations," *IEEE Trans. Power Del.*, vol. 24, no. 3, pp. 1490–1503, Jul. 2009.
- [10] E. Martinez, I. Fernandez, and J. M. Canales, "Thyristor based solid state tap changer for distribution transformers," in *Proc. IEEE 11th Int. Workshop Electron., Control, Meas., Signals Appl. Mechatronics*, Toulouse, France, 2013, pp. 1–5.
- [11] H. Ma, S. Gu, H. Wang, H. Xu, C. Wang, and H. Zhou, "On-load automatic voltage regulation system designed via thyristor for distribution transformer," in *Proc. 20th Int. Conf. Elect. Mach. Syst.*, 2017, pp. 1–5, doi: [10.1109/ICEMS.2017.8055967](https://doi.org/10.1109/ICEMS.2017.8055967).
- [12] J. Faiz and B. Siahkollah, "New solid-state on-load tap-changers topology for distribution transformers," *IEEE Trans. Power Del.*, vol. 18, no. 1, pp. 136–141, Jan. 2003.
- [13] J. de Oliveira Quevedo et al., "Analysis and design of an electronic on-load tap changer distribution transformer for automatic voltage regulation," *IEEE Trans. Ind. Electron.*, vol. 64, no. 1, pp. 883–894, Jan. 2017.
- [14] N. Chen and L. E. Jonsson, "A new hybrid power electronics on-load tap changer for power transformer," in *Proc. IEEE Appl. Power Electron. Conf. Expo.*, Charlotte, NC, USA, 2015, pp. 1030–1037.
- [15] G. R. Chandra Mouli, P. Bauer, T. Wijekoon, A. Panosyan, and E.-M. Bärthlein, "Design of a power-electronic-assisted OLTC for grid voltage regulation," *IEEE Trans. Power Del.*, vol. 30, no. 3, pp. 1086–1095, Jun. 2015.
- [16] D. J. Rogers and T. C. Green, "An active-shunt diverter for on-load tap changers," *IEEE Trans. Power Del.*, vol. 28, no. 2, pp. 649–657, Apr. 2013.
- [17] C. Kumar and M. Liserre, "Operation and control of smart transformer for improving performance of medium voltage power distribution system," in *Proc. IEEE 6th Int. Symp. Power Electron. Distrib. Gener. Syst.*, Aachen, Germany, 2015, pp. 1–6.
- [18] Q. Zhu, L. Wang, A. Q. Huang, K. Booth, and L. Zhang, "7.2-kV single-stage solid-state transformer based on the current-fed series resonant converter and 15-kV SiC mosfets," *IEEE Trans. Power Electron.*, vol. 34, no. 2, pp. 1099–1112, Feb. 2019, doi: [10.1109/TPEL.2018.2829174](https://doi.org/10.1109/TPEL.2018.2829174).
- [19] D. Dong, M. Agamy, J. Z. Bebic, Q. Chen, and G. Mandrusiak, "A modular SiC high-frequency solid-state transformer for medium-voltage applications: Design, implementation, and testing," *IEEE J. Emerg. Sel. Topics Power Electron.*, vol. 7, no. 2, pp. 768–778, Jun. 2019, doi: [10.1109/JESTPE.2019.2896046](https://doi.org/10.1109/JESTPE.2019.2896046).
- [20] A. Q. Huang, Q. Zhu, L. Wang, and L. Zhang, "15 kV SiC MOSFET: An enabling technology for medium voltage solid state transformers," *CPSS Trans. Power Electron. Appl.*, vol. 2, no. 2, pp. 118–130, 2017, doi: [10.24295/CPSSSTPEA.2017.00012](https://doi.org/10.24295/CPSSSTPEA.2017.00012).
- [21] T. Guillod, F. Krismer, and J. W. Kolar, "Protection of MV converters in the grid: The case of MV/LV solid-state transformers," *IEEE J. Emerg. Sel. Topics Power Electron.*, vol. 5, no. 1, pp. 393–408, Mar. 2017, doi: [10.1109/JESTPE.2016.2617620](https://doi.org/10.1109/JESTPE.2016.2617620).
- [22] J. E. Huber and J. W. Kolar, "Applicability of solid-state transformers in today's and future distribution grids," *IEEE Trans. Smart Grid*, vol. 10, no. 1, pp. 317–326, Jan. 2019.
- [23] X. She, A. Q. Huang, and R. Burgos, "Review of solid-state transformer technologies and their application in power distribution systems," *IEEE J. Emerg. Sel. Topics Power Electron.*, vol. 1, no. 3, pp. 186–198, Sep. 2013.
- [24] S. A. Saleh et al., "Solid-state transformers for distribution systems—Part II: Deployment challenges," *IEEE Trans. Ind. Appl.*, vol. 55, no. 6, pp. 5708–5716, Nov./Dec. 2019, doi: [10.1109/TIA.2019.2938143](https://doi.org/10.1109/TIA.2019.2938143).
- [25] M. A. Hannan et al., "State of the art of solid-state transformers: Advanced topologies, implementation issues, recent progress and improvements," *IEEE Access*, vol. 8, pp. 19113–19132, 2020, doi: [10.1109/ACCESS.2020.2967345](https://doi.org/10.1109/ACCESS.2020.2967345).
- [26] J. Kaniewski, P. Szczesniak, M. Jarnut, and G. Benysek, "Hybrid voltage sag/swell compensators: A review of hybrid AC/AC converters," *IEEE Ind. Electron. Mag.*, vol. 9, no. 4, pp. 37–48, Dec. 2015.
- [27] T. Kang, S. Choi, A. S. Morsy, and P. N. Enjeti, "Series voltage regulator for a distribution transformer to compensate voltage sag/swell," *IEEE Trans. Ind. Electron.*, vol. 64, no. 6, pp. 4501–4510, Jun. 2017, doi: [10.1109/TIE.2017.2668982](https://doi.org/10.1109/TIE.2017.2668982).
- [28] S. Giacomuzzi, M. Langwasser, G. De Carne, G. Buja, and M. Liserre, "Smart transformer-based medium voltage grid support by means of active power control," *CES Trans. Elect. Mach. Syst.*, vol. 4, no. 4, pp. 285–294, Dec. 2020, doi: [10.30941/CESTEMS.2020.00035](https://doi.org/10.30941/CESTEMS.2020.00035).
- [29] P. Kou, D. Liang, R. Gao, Y. Liu, and L. Gao, "Decentralized model predictive control of hybrid distribution transformers for voltage regulation in active distribution networks," *IEEE Trans. Sustain. Energy*, vol. 11, no. 4, pp. 2189–2200, Oct. 2020, doi: [10.1109/TSTE.2019.2952171](https://doi.org/10.1109/TSTE.2019.2952171).
- [30] M. Chamana and B. H. Chowdhury, "Optimal voltage regulation of distribution networks with cascaded voltage regulators in the presence of high PV penetration," *IEEE Trans. Sustain. Energy*, vol. 9, no. 3, pp. 1427–1436, Jul. 2018, doi: [10.1109/TSTE.2017.2788869](https://doi.org/10.1109/TSTE.2017.2788869).
- [31] X. Gao, F. Sossan, K. Christakou, M. Paolone, and M. Liserre, "Concurrent voltage control and dispatch of active distribution networks by means of smart transformer and storage," *IEEE Trans. Ind. Electron.*, vol. 65, no. 8, pp. 6657–6666, Aug. 2018, doi: [10.1109/TIE.2017.2772181](https://doi.org/10.1109/TIE.2017.2772181).
- [32] L. Zheng et al., "Solid-state transformer and hybrid transformer with integrated energy storage in active distribution grids: Technical and economic comparison, dispatch, and control," *IEEE J. Emerg. Sel. Topics Power Electron.*, vol. 10, no. 4, pp. 3771–3787, Aug. 2022, doi: [10.1109/JESTPE.2022.3144361](https://doi.org/10.1109/JESTPE.2022.3144361).
- [33] Y. Liu et al., "Compound control system of hybrid distribution transformer," *IEEE Trans. Ind. Appl.*, vol. 56, no. 6, pp. 6360–6373, Nov./Dec. 2020, doi: [10.1109/TIA.2020.3014058](https://doi.org/10.1109/TIA.2020.3014058).
- [34] H.-J. Lee and Y.-D. Yoon, "Intelligent transformer unit topology using additional small power converter based on conventional distribution transformer," in *Proc. IEEE Energy Convers. Congr. Expo.*, 2019, pp. 4639–4645, doi: [10.1109/ECCE.2019.8912672](https://doi.org/10.1109/ECCE.2019.8912672).
- [35] D. Das, R. P. Kandula, J. A. Muñoz, D. Divan, R. G. Harley, and J. E. Schatz, "An integrated controllable network transformer—Hybrid active filter system," *IEEE Trans. Ind. Appl.*, vol. 51, no. 2, pp. 1692–1701, Mar./Apr. 2015, doi: [10.1109/TIA.2014.2350081](https://doi.org/10.1109/TIA.2014.2350081).

- [36] H. Chen, A. R. Iyer, R. G. Harley, and D. Divan, "Dynamic grid power routing using controllable network transformers (CNTs) with decoupled closed-loop controller," *IEEE Trans. Ind. Appl.*, vol. 51, no. 3, pp. 2361–2372, May/Jun. 2015, doi: [10.1109/TIA.2014.2379917](https://doi.org/10.1109/TIA.2014.2379917).
- [37] "Datasheet I. K. Q.120N.60T," Infineon Technol., Neubiberg, Germany, 1999–2021. [Online]. Available: https://www.infineon.com/dgdl/Infineon-IKQ120N60T-DS-v02_03-EN.pdf?fileId=5546d46249cd10140149d230bd094df7
- [38] Y. Wang, T. Zhao, M. Rashidi, J. Schaar, and A. Trujillo, "An arcless step voltage regulator based on series-connected converter for branch current suppression," *IEEE J. Emerg. Sel. Topics Power Electron.*, vol. 9, no. 5, pp. 5272–5281, Oct. 2021, doi: [10.1109/JESTPE.2020.2989164](https://doi.org/10.1109/JESTPE.2020.2989164).
- [39] P. G. Slade, *Electrical Contacts: Principles and Applications*. New York, NY, USA: Taylor & Francis, 1999.



YAFENG WANG (Member, IEEE) received the B.S. degree in electrical engineering from the Harbin Institute of Technology, Harbin, China, in 2015, the M.S. degree in electrical and computer engineering from Ohio State University, Columbus, OH, USA, in 2017, and the Ph.D. degree in electrical and computer engineering from the University of North Carolina at Charlotte, Charlotte, NC, USA, in 2021.

From 2017 to 2021, he was with Renewable Energy and Power Electronics Advanced Research

Lab and Energy Production and Infrastructure Center, University of North Carolina at Charlotte, Charlotte, NC, USA. He is currently a Senior Applications Engineer with Monolithic Power Systems, Inc., San Jose, CA, USA. His research interests include grid-edge power electronics and voltage regulators.



TIEFU ZHAO (Senior Member, IEEE) received the B.S. and M.S. degrees from Tsinghua University, Beijing, China, in 2003 and 2005, respectively, and the Ph.D. degree from North Carolina State University, Raleigh, NC, USA, in 2010, all in electrical engineering.

From 2010 to 2016, he was with Eaton Corporation Research and Technology, Milwaukee, WI, USA. He is currently an Associate Professor with the Department of Electrical and Computer Engineering and the Energy Production and Infra-

structure Center, University of North Carolina at Charlotte, Charlotte, NC, USA. He has authored or coauthored more than 60 papers in refereed journals and international conference proceedings. He has 12 patents awarded. His current research interests include solid-state transformer, solid-state circuit protection, wireless power transfer, wide bandgap device-based power conversion, power electronics reliability, and fault detection.

Dr. Zhao was the recipient of 2015 IAS Andrew W. Smith Outstanding Young Member Award, 2015 STEM Forward Young Engineer of the Year Award, and Prize Paper Awards from the IEEE ECCE 2020 and ITEC 2021. His Ph.D. research on solid-state transformer was named the world's top ten emerging technologies by MIT technology review 2011. He was an Associate Editor for the IEEE JOURNAL OF EMERGING AND SELECTED TOPICS IN POWER ELECTRONICS. He has served as the Organizing Committee Member on several international conferences, including ECCE 2016–2019 and PEDG 2018. He is the Founding Chair of the IEEE Charlotte section PELS/IAS/IES Chapter.